Eur Biophys J (1993) 22:269–277

European Biophysics Journal


# Hydrophilic surface maps of channel-forming peptides: analysis of amphipathic helices

**Ian D. Kerr, Mark S. P. Sansom**

Laboratory of Molecular Biophysics, University of Oxford, Rex Richards Building, South Parks Road, Oxford OX1 3QU, UK

Received: 19 February 1993 / Accepted in revised form: 27 May 1993

**Abstract.** Ion channels may be formed by bundles of amphipathic α-helices aligned parallel to one another and spanning a lipid bilayer membrane, with the hydrophilic faces of the helices lining a central pore. In order to provide insight into the packing of such helices in bundles, a method has been developed to evalute *hydrophilic surface maps* of amphipathic α-helices and to display these surfaces in a readily interpretable form. The procedure is based upon empirical energy calculations of interactions of a water molecule with an amphipathic α-helix. The method has been applied to three channel-forming peptides: *Staphylococcal* δ-toxin; alamethicin; and a synthetic leucine- and serine-containing peptide. Particular emphasis is placed upon the effects of sidechain conformational flexibility on hydrophilic surface maps. A family of models of the δ-toxin helix is generated by a simulated annealing procedure. The results of hydrophilic surface map analyses provide more exact definition of the centre of the hydrophilic face of amphipathic helices, and of the variation of the position of the centre in response to changes in sidechain conformation. This information is used to define *families* of preliminary models for a given ion channel, as is illustrated for δ-toxin.

**Key words:** Amphipathic α-helix – Channel-forming peptide – Hydrophilic surface map – Membrane protein – Simulated annealing

## Introduction

Channel-forming peptides (CFPs) are model ion channels which mimic many of the functional properties of larger and more complex channel proteins. X-ray and NMR structures of CFPs reveal that they form amphipathic α-helices. Ion channes may be formed by bundles of parallel CFP helices (Lear et al. 1988; Sansom 1991), as is illustrated in Fig. 1 A. The helices are oriented perpendicular to the plane of the membrane, and are arranged about a central pore so as to form an assembly with cyclic symmetry about the pore axis. The hydrophilic sidechains of the helices line the central pore, whilst the hydrophobic sidechains interact favourably with the fatty acyl chains of bilayer lipids. Consequently, such assemblies are stabilized by peptide-peptide, peptide-water and peptide-lipid interactions, and also by the interaction of peptide molecular dipoles with the transbilayer electrostatic field. Parallel bundles of transbilayer α-helices constitute a structural motif present in several ion channel proteins (Oiki et al. 1990). This motif is of particular importance with respect to the members of the nAChR superfamily, the central pores of which are believed to be formed by a bundle of five parallel amphipathic helices (Unwin 1989; Stroud et al. 1990; Sansom 1992a). Its presence in other ion channel proteins, e.g. the influenza $M_2$ channel (Sansom and Kerr 1993), suggests that the helix bundle motif is of general importance. In order to develop molecular models of such transbilayer pores it is essential that the amphipathic nature of CFPs is examined in some depth.

In modelling pore formation by CFPs a necessary initial step is to identify the centre of the hydrophilic face of an amphipathic helix in order that this face may be oriented towards the centre of a helix bundle (Sansom et al. 1991; Fig. 1 A). This provides a water-like environment within the pore allowing possible transient interactions with permeant ions (Sansom et al. 1993). However, it is not clear exactly how to define the centre of the hydrophilic face of an amphipathic helix. In particular, an estimate of the variation in the position of the centre would enable construction of a range of initial channel models for refinement and further analysis.

An amphipathic α-helix is defined as one with an asymmetric distribution of polar and apolar residues between opposite sides of the helix. Previously, identification of helix amphipathicity has employed qualitative

*Abbreviations:* ABNR, adopted basis Newton-Raphson; CFP, channel-forming peptide; HSM, hydrophilic surface map; MHP, molecular hydrophobicity potential; RMSD, root mean square deviation

*Correspondence to:* M. S. P. Sansom

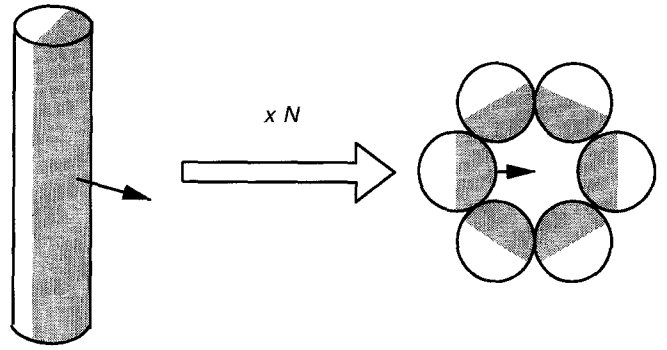


A

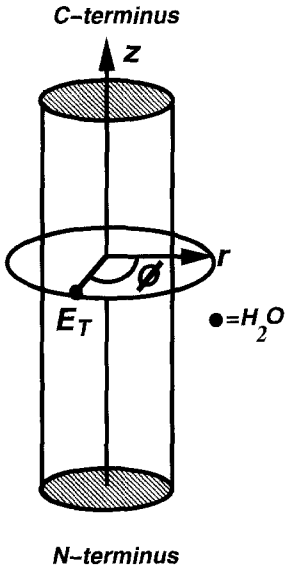


B

**Fig. 1.** **A** Diagram of bundle formation by amphipathic helices. The cylinder represents an α-helix with the hydrophilic face shaded, and the arrow designating the centre of this face. N = 6 such helices assemble to form a helix bundle surrounding a central pore. **B** Coordinate system used in empirical energy calculations of the interaction of a water molecule with an α-helix. The cyclindrical polar grid is defined by $z$, $r$ and $\phi$ where $z$ is coincident with the helix axis, $r$ is the distance from the helix centre and $\phi$ is the angle subtended in the $(z, r)$ plane

methods such as helical wheel plots (Schiffer and Edmundson 1967) or quantitative procedures such as calculation of mean hydrophobic moments (Eisenberg et al. 1982; Eisenberg 1984). The helical wheel is a projection down the helix axis of the Cα atoms of an α-helix. Asymmetric distribution of hydrophobic and hydrophilic residues on this projection (identified by eye) is interpreted as amphipathicity. Such asymmetry in the distribution of the hydrophilic and hydrophobic residues may be quantified via calculation of the mean hydrophobic moment, a vector quantity derived by averaging the individual hydrophobic moments of the constituent residues of the helix. However, the exact hydrophilic surface of an amphipathic helix containing *flexible* polar sidechains cannot be determined solely from consideration of α-carbon positions. When high resolution data and/or molecular models are available, it is possible to analyze helix amphipathicity whilst taking into consideration possible alternative conformations of sidechains.

We employ a procedure for calculation of the interaction energy of a water molecule with an amphipathic α-helix which enables display of the results as a *hydrophilic surface* map. This representation is sensitive to changes in sidechain conformation. Molecular dynamics based modelling procedures may be used to generate *families* of structures for CFP monomers, which thus provide estimates of sidechain flexibility. Hydrophilic surface maps calculated for representative structures from such families may be used to define the range of values for the centre of the hydrophilic face of an α-helix. This information in turn may be employed to generate families of initial models of ion channels formed by bundles of parallel amphipathic helices.

We have investigated three examples of amphipathic CFPs for which structural information of differing resolution is available: (*a*) *Staphylococcus aureus* δ-toxin; (*b*) alamethicin; and (*c*) a synthetic leucine- and serine-containing CFP designed by Lear et al. (1988). Taken together, these provide a thorough analysis of the effects of polar sidechain flexibility on definition of hydrophilic surfaces and on construction of initial models of ion channels.

## Methods

### *General computational methods*

Molecular modelling was performed using Quanta 3.2 (Polygen, Waltham, MA) and CHARMm (V21.3; Brooks et al. 1983) running on a Silicon Graphics (Mountain View, CA) Indigo Workstation. Molecular dynamics simulations were carried out using Xplor 3.0 (Brünger 1992). Structure diagrams were generated using MolScript (Kraulis 1991). All auxiliary programs were written in Fortran 77.

### *Modelling of monomers*

Interactive modelling of helical monomers was carried out as described in Sansom and Kerr (1993). Mainchain torsion angles for a right-handed α-helix ($\phi = -66°$, $\psi = -40°$) were those obtained by analysis of the crystal structures of 60 proteins solved to a resolution of 2.0 Å or less (McGregor et al. 1987). The $\chi_1$ and $\chi_2$ torsion angles for all sidechains (except $\chi_1$ of serine residues – see below) were set to the preferred conformation in an α-helical structure as reported by various authors (Janin et al. 1978; McGregor et al. 1987; Richardson and Richardson 1989). The model thus obtained was subjected to 1 000 cycles of ABNR (adopted basis Newton-Raphson) energy minimisation with the Cα atoms constrained in order to retain the overall helix geometry.

Simulated annealing was performed as described by Nilges et al. (1988) and by Nilges and Brünger (1991).

### *Hydrophilic surface maps*

Hydrophilic surface maps (HSMs) were generated by placing a water molecule at successive positions on a

cylindrical polar grid around a peptide molecule, and evaluating the peptide-water interaction energy. The water model employed was TIP3P (Jorgensen et al. 1983) which provides a reasonable representation of the physicochemical properties of liquid water while retaining a relatively simple, three-point charge model.

The cylindrical polar grid is defined by three coordinates $z$, $r$ and $\phi$ (Fig. 1B), where $z$ is coincident with the helix axis, $r$ is the distance from the centre of the helix axis and $\phi$ is the angle subtended in the $(z, r)$ plane. The $z$-axis is defined as being a line drawn between two dummy atoms, one at the midpoint of all the Cα atoms of the helix, the other at the midpoint of the four C-terminal Cα atoms. This definition is modified for peptides, e.g. alamethicin, which contain a proline-induced kink in the helix (see below). Typically $z$ and $r$ are incremented in 1 Å steps, and $\phi$ in 10° steps, corresponding to approximately 20 000 grid points for $z = -25$ to $+2.5$ Å.

At each grid point $(z, r, \phi)$ an energy minimisation is performed in order to optimise the orientation of the hydrogen atoms of the water molecule. The helix atoms and the oxygen of the water molecule are fixed and the hydrogen atoms subjected to 1 000 cycles of adopted base Newton-Raphson (ABNR) energy minimsation. After minimisation, the energy of the helix and water molecule ($E_T$) is calculated as the sum of the van der Waals and electrostatic energies. The interaction energy, $E_{int}$, between the water probe and the helix is defined as being the difference between $E_T(z, r, \phi)$ and $E_T$ when the water molecule is distant from the peptide e.g. typically at $z = +50$ Å. For each value of $(z, \phi)$, the minimum of $E_{int}$ with respect to $r$ is determined. This thus defines an $E_{min}(z, \phi)$ surface, i.e. the hydrophilic surface map, which can be displayed as a contour plot of isopotential lines for the helix-water interaction energy. Averaging $E_{min}(z, \phi)$ over all $z$ values for the length of the helix generates a plot of $\langle E_{min} \rangle$ vs. $\phi$ which may then be used to identify the centre of the hydrophilic face of the helix.

## Results

### *δ-Toxin*

The 26 residue peptide δ-toxin from *Staphylococcus aureus* (Fitton 1981; Table 1) has been the subject of detailed investigations of its physicochemical properties and secondary structure. The results of both proton NMR (Lee et al. 1987; Tappin et al. 1988) and circular dichroism (Fitton 1981; Thiaudière et al. 1991), suggest that the peptide is α-helical from residues 1–20, with a rather more flexible C-terminal hexapeptide. Planar bilayer studies of channel formation by this peptide (Mellor et al. 1988) suggest that, on average, six transbilayer helices form a weakly cation selective pore.

The NMR studies of δ-toxin do not provide detailed information on sidechain conformations. Simulated annealing techniques have therefore been used to generate a family of model structures. This approach has recently been employed by Nilges and Brünger (1991; 1993) to construct, ab initio, models of leu-zipper helix dimers, and by Treutlein et al. (1992) to model the glycophorin A transmembrane domain dimer. We have also used this method to model helices formed by H5 (Haris et al. 1993) and S4 (Breed et al., unpublished results) synthetic peptides derived from the *Shaker* $K^+$ channel protein.

**Table 1.** Amino acid sequences of CFPs

| Peptide | Sequences |
|---|---|
| δ-toxin | f-M-A-**Q**-**D**-I-I-**S**-**T**-I-G-**D**-L-V-**K**-W-I-I-**D**-**T**-V-**N**-**K**-F-**T**-**K**-**K** |
| alamethicin | Ac-U-*P*-U-A-U-A-**Q**-U-V-U-G-L-U-*P*-V-U-U-**E**-**Q**-F-OH |
| LS1 | L-S-S-L-L-S-L-L-S-S-L-L-S-L-L-S-S-L-L-S-L-L-S-L-$NH_2$ |

The standard single letter code is used with the addition of U = α-amino isobutyric acid. Polar residues are denoted by bold typeface, proline by italics. The following abbreviations are used for terminal and blocking groups: Ac-acetyl; f-formyl; $NH_2$-C terminal amide

An initial model was constructed by placing the 26 Cα atoms of δ-toxin at their positions in an idealised α-helix. The remaining non-Cα atoms were superimposed upon the Cα atoms of their corresponding residues. This model was used as the basis of 5 independent simulated annealing runs in which sidechain and non-Cα mainchain atoms were allowed to "grow out" from their Cα atoms. The positions of the Cα atoms remained fixed throughout the run. The simulated annealing started at 1000 K. Maintaining this temperature for 11.5 ps, bond geometry and planarity scaling factors were gradually increased, with the latter lagging behind the former. A repulsive van der Waals term was then gradually introduced over a further 21 ps at 1 000 K. The temperature was then reduced in a stepwise manner to 300 K over a period of 8.4 ps. An electrostatic term was *not* included during the simulated annealing, which thus was driven by bond geometries and steric interactions.

The resultant 5 models were each subjected to 5 dynamics runs, resulting in 25 final δ-toxin models. Each dynamics run was divided into two phases. Phase one consisted of a limited additional simulated annealing run, from 500 K to 300 K over 4 ps, during which the electrostatics term was gradually switched on by scaling of polar sidechain atom charges. The initial scale factor was 0.05, rising to a final value of 0.42. During this phase, initial harmonic constraints on Cα atom positions were gradually relaxed. Phase two consisted of 5 ps of unrestrained dynamics, during which Cα atoms were free, whilst backbone hydrogen bonds were weighted by an additional factor of 2.5. The resultant models were finally subjected to 1 000 cycles of conjugate gradient minimisation.

Analysis of the final models (Fig. 2) using Procheck (Morris et al. 1992) confirmed that the stereochemistry of the models was consistent with that found in highly refined crystallographic structures of proteins. Ramachandran plot analysis showed that all backbone torsion angles fell within the allowed region for a right-handed α-helix. The overall RMSD between the 25 models was 1.95 Å for all non-H atoms, and 1.14 Å for backbone atoms. The residue by residue RMSDs (Fig. 2C) were

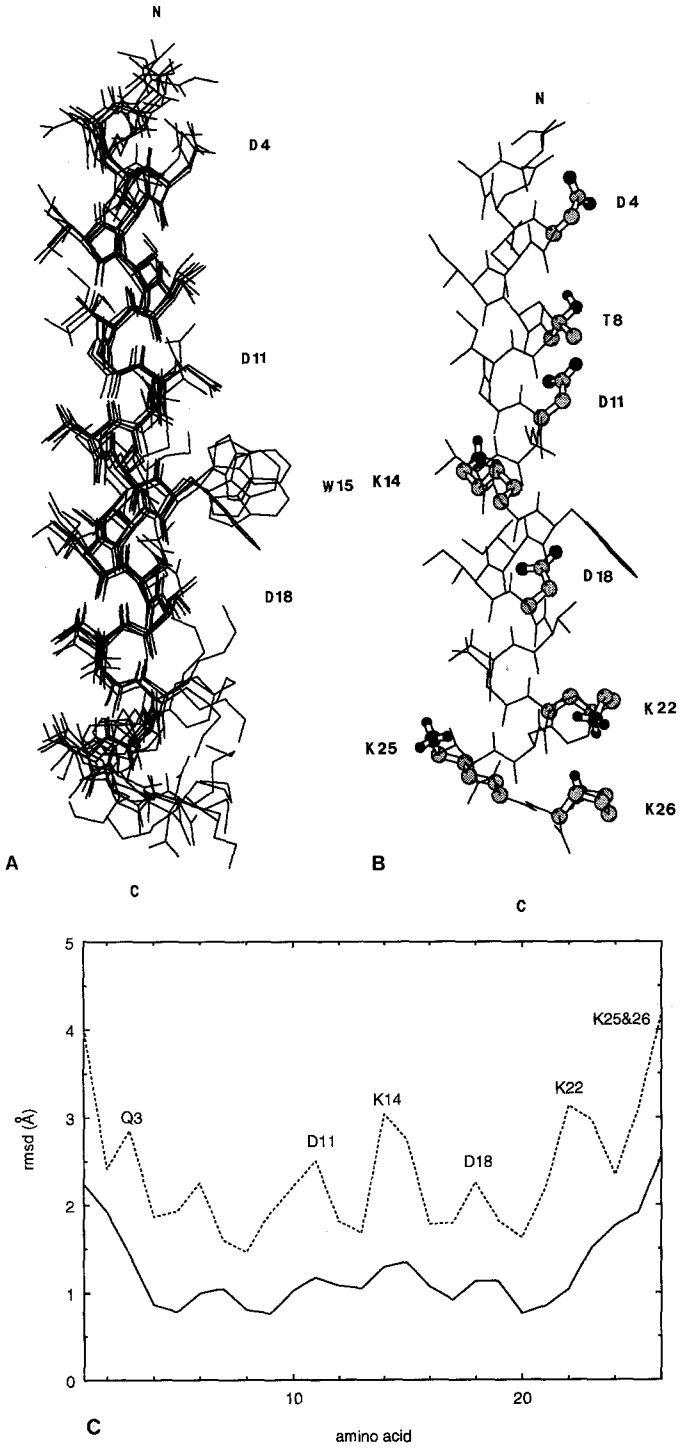


**Fig. 2.** **A** Five randomly selected models of the δ-toxin α-helix superimposed. **B** Single representative model of δ-toxin. Sidechains D4, T8, D11, D18, K23, K25 and K26 are displayed in "ball-and-stick" format. **C** RMSD vs. residue number for the 25 δ-toxin models compared. The solid line corresponds to backbone (non-H) atoms and the dotted line to sidechain atoms

larger at the helix termini than in the centre, as has been observed in several molecular dynamics studies of α-helices (e.g. Levy et al. 1982). Detailed comparison of the 25 models reveals that there is considerable flexibility in sidechain conformations whilst the helical backbone geometry is conserved. In particular residues Q3, D11, K14, D18 and K22 correspond to peaks in the RMSD vs. residue plot and thus exhibit greater conformational heterogeneity than the remaining sidechains. Five models were selected at random from the final 25 for HSM analysis. It is evident from examination of Fig. 2A that *inter alia* these models include alternative conformations for the three aspartate sidechains, and for the two C-terminal lysines.

The hydrophilic surface map for the δ-toxin model shown in Fig. 2B is illustrated in Fig. 3A as a contour plot. Energy minima are clearly visible corresponding to favourable interactions of the sidechains of residues D4, D11 and D18 with water. There is also a broad minimum corresponding to the cluster of lysine residues at the C-terminus. Figure 3B shows the $\langle E \rangle$ vs. $\phi$ plots for the 5 selected models. It is clear that the definition of the centre of the hydrophilic face of the helix varies from ca. $\phi = +40°$ to $\phi = +60°$, i.e. a range of 20°. This reflects variation in the conformations of the charged (aspartate and lysine) sidechains between the five different models. The mean $\langle E \rangle$ vs. $\phi$ curve is shown in Fig. 3C. There is a distinct minimum at $\phi = +50°$, representing the centre of the hydrophilic face of the helix, and a shoulder at $\phi = +130°$. The minimum ($\phi = +50°$) corresponds to the position on $\phi$ of residues D11 and D18, whereas the shoulder ($\phi = +130°$) corresponds to T8 and T19.

This definition of the centre of the hydrophilic face, in terms of mean value and range, is illustrated in Fig. 4, alongside the initial channel model thus generated, in which a hexameric bundle of parallel helices, each rotated about its long axis by $\phi = +50°$, has been constructed. The central pore is lined by the sidechains of residues D4, D11 and D18. A range of models, corresponding to the range of $\phi$ values noted above, may therefore be constructed and used as the basis of attempts to refine the initial channel models using simulated annealing procedures similar to those discussed above (Kerr and Sansom, unpublished results).

## *Alamethicin*

The channel-forming and conformational properties of alamethicin, a 20 residue peptaibol isolated from *Trichoderma viride* have been studied intensively over the past two decades (reviewed by Sansom 1991, 1993; Woolley and Wallace 1992). The crystal structure of alamethicin, determined to 1.5 Å resolution (Fox and Richards 1982), contains three monomers in the asymmetric unit (A, B and C) which differ mainly in the conformation of the E18 sidechain. These provide an opportunity to investigate the effect of changes in the conformation of a single charged sidechain on hydrophilic surface maps. The alamethicin coordinates were taken from entry 1AMT of the Brookhaven protein data bank (Bernstein et al. 1977). The three monomers were aligned prior to evaluating their hydrophilic surface maps by least squares superimposition of their backbone atoms. Alamethicin contains a proline residue at position 14 (Table 1) which results in a kink in the helix. It is therefore not possible to define *z* as being coincident with a single axis. In order to circum-

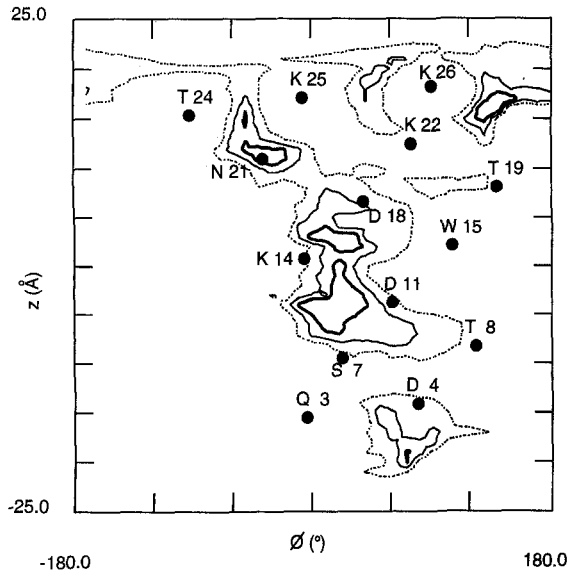


A

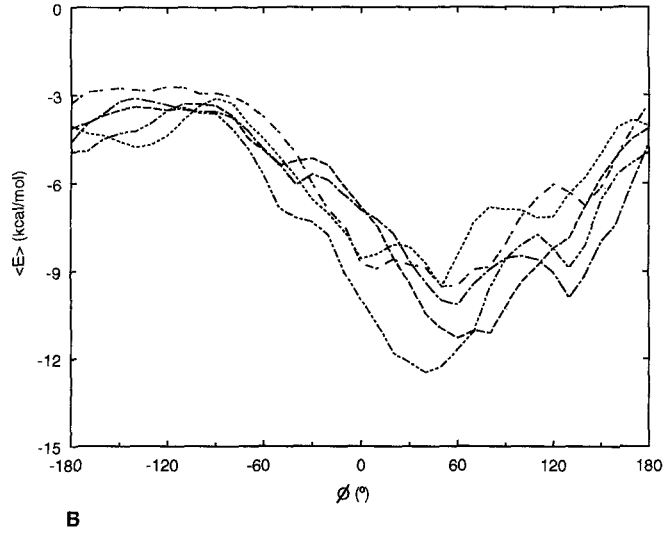


B

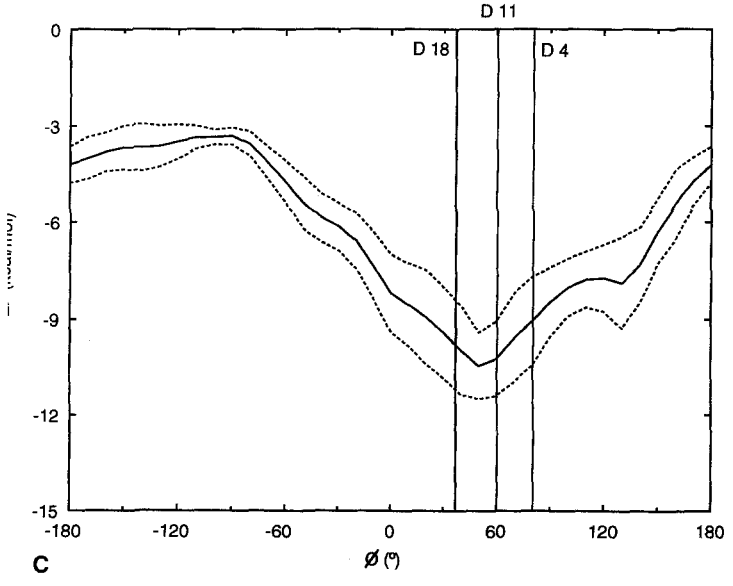


C

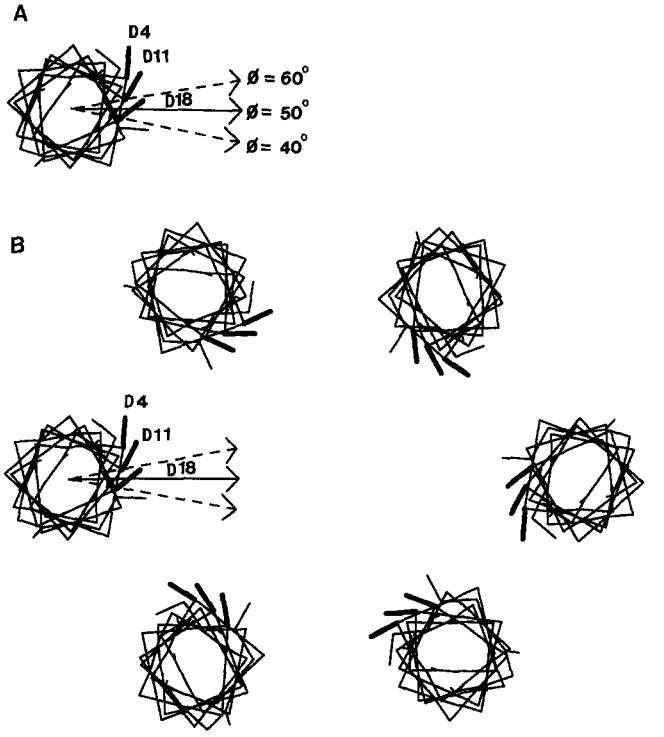


**Fig. 4.** **A** Diagram of the range of values of $\phi$ (from $+40°$ to $+60°$) defining the centre of the hydrophilic face of a $\delta$-toxin helix. The "consensus" value of $\phi = +50°$ is indicated by the solid arrow. The $\delta$-toxin monomer is shown as the helix backbone atoms with the addition of bold lines to indicate the C$\alpha$-C$\beta$ bonds of the D4, D11 and D18 residues. **B** Preliminary model of a $\delta$-toxin channel. A hexameric bundle of $\delta$-toxin helices was constructed with an inter-helical distance of 10.5 Å. The helices are oriented such that the "consensus" definition of the centre of the hydrophilic face is directed towards the centre of the pore. The channel-lining aspartate residues are indicated. The arrows represents the hydrophilic face as in **A**

vent this, the hydrophilic surface was evaluated in two halves, one in which $z$ was coincident with the axis of the N-terminal helix (residues 1 to 14) and one in which $z$ was coincident with the axis of the C-terminal helix (residues 13 to 20; Fig. 5A). The resultant hydrophilic surface maps are thus composed of two sections, one for each helical segment. The boundary between the two sections corresponds to the position, on $z$, of the C$\alpha$ atom of residue G11. Figure 5B displays the hydrophilic surface map for molecule B of the alamethicin structure. This monomer was subjected to 50 cycles of steepest descents energy minimisation prior to evaluation of peptide-water interactions in order to resolve any minor stereochemical

**Fig. 3.** **A** Hydrophilic surface maps for the $\delta$-toxin model shown in Fig. 2B. The HSM is depicted as isopotential lines at $-10$ (*dotted line*), $-15$ (*solid line*) and $-20$ (*bold line*) kcal/mol. The positions of selected C$\alpha$ atoms are superimposed on the contour map. **B** shows the result of averaging the interaction energy over all values of $z$ in order to yield $\langle E_{min} \rangle$ vs. $\phi$ (see text). A minimum in such a curve defines the centre of the hydrophilic face of an $\alpha$-helix. The $\langle E_{min} \rangle$ vs. $\phi$ curves for the five models shown in Fig. 2A are superimposed. **C** is the mean ($\pm$SD) of the $\langle E_{min} \rangle$ vs. $\phi$ curves in **B**. The positions, on $\phi$, of the C$\alpha$ atoms of the three aspartate residues are indicated by vertical lines

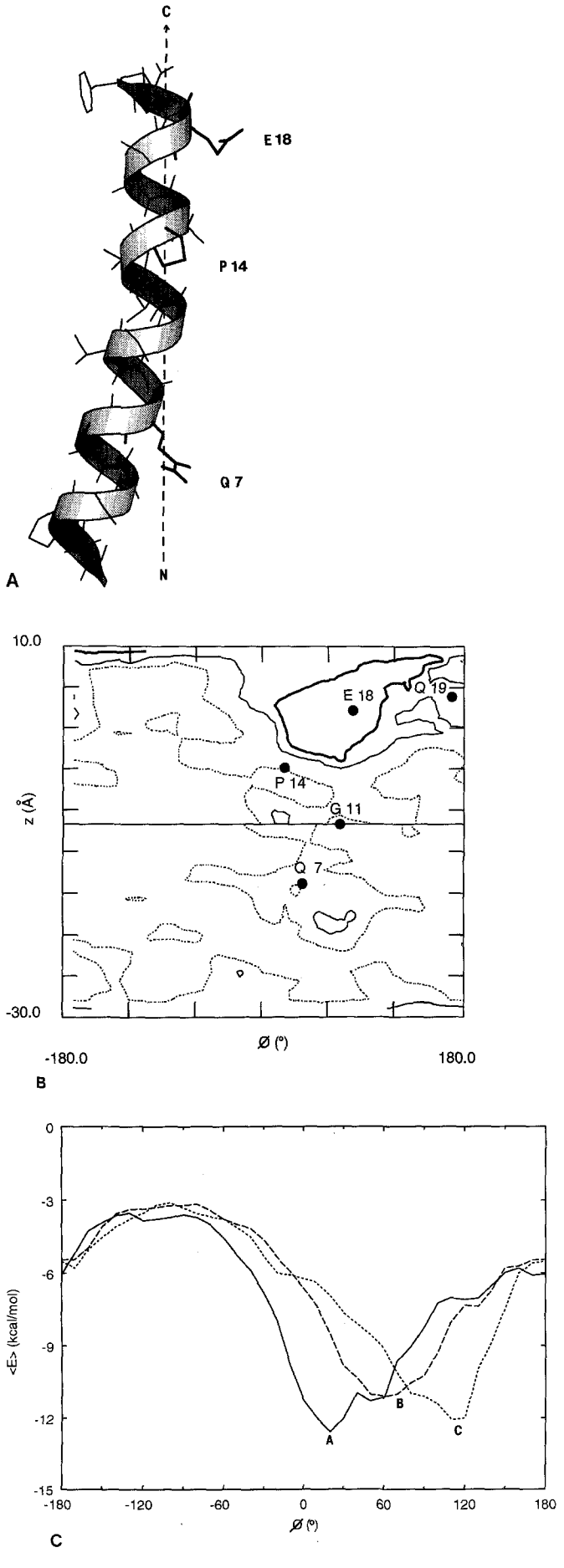


conflicts. The most hydrophilic area is that around E18 at the C-terminus, but there is also a hydrophilic patch in the vicinity of Q7. The corresponding graphs of $\langle E_{min} \rangle$ vs. $\phi$ for the two halves of the molecule reveal that the centre of the hydrophilic face of alamethicin lies between the position, on $\phi$, of Q7 and E18, at a value of $\phi = +60°$. Notice that the hydrophilic faces thus defined are coincident, on $\phi$, for the N- and C-terminal helices.

Hydrophilic surface maps were also evaluated for molecules A and C from the alamethicin crystal structure in order to investigate the effects of changes in E18 conformation. The plots of $\langle E_{min} \rangle$ vs. $\phi$ for the C-terminal helices of alamethicin molecules A, B and C are superimposed in Fig. 5C. It is evident that the value of $\phi$ defining the centre of the hydrophilic face of the C-terminal helix differs between A ($\phi = 20°$), B ($\phi = 60°$) and C ($\phi = 120°$). The most substantial difference is between A and C. In A, the $\chi_1$ for E18 is $g^+$, whereas in C it is trans ($t$). It is interesting to note that the crystallographic B factor for the sidechain atoms of E18 is somewhat higher in monomer C than in A and B. The extended conformation of E18 in molecule C allows a water molecule to interact favourably with E18 and Q19 simultaneously. This shifts the position of the most hydrophilic "patch" of the surface to a higher value of $\phi$, hence the resultant change in the $\phi$ value defining the centre of the hydrophilic face.

This analysis of the C-terminal helix of alamethicin reveals that the centre of the hydrophilic face may vary by about 100°, depending on the conformation of E18. This suggests that in refining models of alamethicin helix bundles in which the C-terminal helices are close packed (Fox and Richards 1982; Sansom 1993) a range of initial models should be evaluated.

### *Synthetic CFP*

Conformational flexibility of serine and threonine sidechains is of particular interest given the presence of these residues in the pore lining of the nicotinic acetylcholine receptor (Villaroel et al. 1991) and related channels. Recent modelling studies suggest that transient interactions of a permeant ion with the lining of such an ion channel may depend upon the conformation of the hydroxylated sidechains (Sansom 1992b). Lear et al. (1988) designed and synthesised a leucine and serine containing peptide (LS1, Table 1) which formed monovalent cation selective ion channels, and which provides an opportunity to investigate such effects. LS1 is based upon a heptad

**Fig. 5.** Hydrophilic surface maps for alamethicin. **A** The structure of alamethicin aligned with the C-terminal helix axis parallel to $z$. Bold lines indicate residues Q7, P14 and E18. The arrow indicates the positive direction of $z$. **B** Hydrophilic surface map of alamethicin. The contour plot is superimposed on the position of selected Cα atoms. The contour levels are in −4 kcal/mol increments from −4 (*dotted line*) to −12 (*bold line*). The horizontal line passing through the Cα position of glycine 11 indicates where the two halves of the surface map are joined. **C** Superimposition of the $\langle E_{min} \rangle$ vs. $\phi$ plots for the C-terminal helices of the three alamethicin monomers: A (*solid line*), B (*broken line*) and C (*dotted line*)

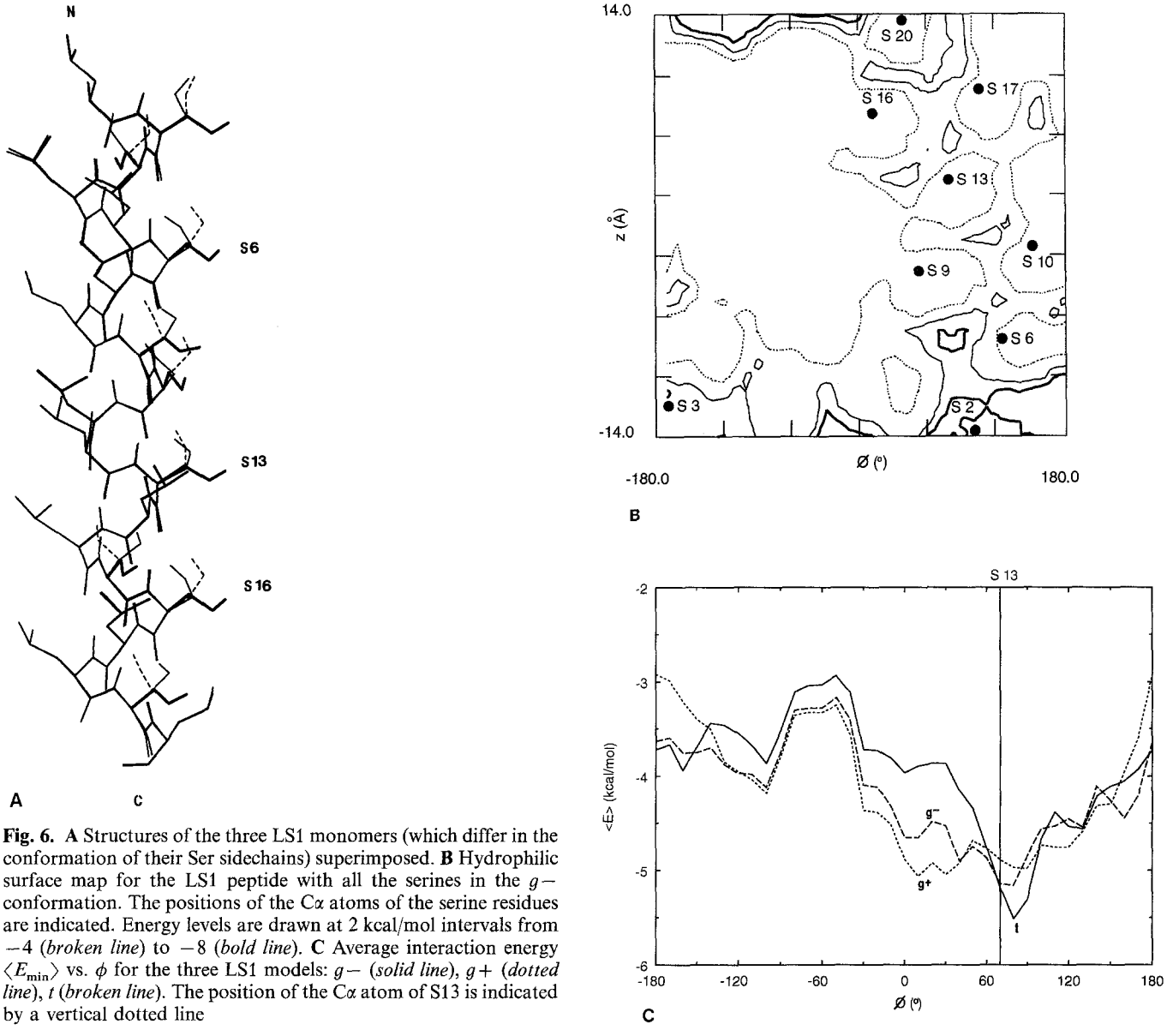


**Fig. 6.** **A** Structures of the three LS1 monomers (which differ in the conformation of their Ser sidechains) superimposed. **B** Hydrophilic surface map for the LS1 peptide with all the serines in the $g-$ conformation. The positions of the Cα atoms of the serine residues are indicated. Energy levels are drawn at 2 kcal/mol intervals from $-4$ (*broken line*) to $-8$ (*bold line*). **C** Average interaction energy $\langle E_{min} \rangle$ vs. $\phi$ for the three LS1 models: $g-$ (*solid line*), $g+$ (*dotted line*), $t$ (*broken line*). The position of the Cα atom of S13 is indicated by a vertical dotted line

repeat motif of leucine and serine residues, and has a blocked C-terminus. CD studies support an α-helical conformation for the peptides (Lear et al. 1988).

The LS peptide enables one to evaluate the effect on helix amphipathicity of hydrogen bonding of hydroxylated sidechains to the peptide backbone (Gray and Matthews 1984; Sansom 1992b). Serine residues may adopt three different conformations in α-helix, $g-$ ($\chi_1 = +60°$), $g+$ ($\chi_1 = -60°$) and $t$ ($\chi_1 = +180°$), with the former two being favoured (Gray and Matthews 1984). Three LS1 models were constructed interactively (Fig. 6A), with all $\chi_1$ for serine set either to $g-$, $g+$ or $t$ and $\chi_2$ set so as to optimise hydrogen bonding. Hydrogen bonding of hydroxyls to the carbonyl oxygen of residues $i$-3 or $i$-4 is present in the $g-$ and $g+$ models but not the $t$ model.

Figure 6B is the HSM corresponding to the LS1 peptide with the serine residues in the $g-$ conformation. The other two models generate similar hydrophilic surfaces. Figure 6C shows the superposition of the $\langle E_{min} \rangle$ vs. $\phi$ plots for the three models, which display different values for the value of $\phi$ corresponding to the centre of the hydrophilic face ($+80°$, ca. $+20°$, and $+80°$ for the $g-$, $g+$ and $t$ conformers respectively). The differences reflect the sensitivity of the definition of the centre of the hydrophilic face to changes in the conformation of hydroxyl-containing sidechains. For example, changing the conformation of a serine sidechain from $g-$ to $g+$ results in rotation of the Oγ atom about the helix axis by ca. 30°, which results in a change in $\phi$ of ca. 50°. Again, this range for the centre of the hydrophilic face results in a family of initial models of LS1 helix bundles for further refinement.

## Discussion

### *Evaluation of hydrophilic surface maps*

The present study was prompted by the need to define hydrophilic surfaces of amphipathic channel-forming helices somewhat more exactly than current methods allow,

in order to guide construction of initial models of ion channels formed by helix bundles. Helical wheel plots (Schiffer and Edmundson 1967), evaluation of hydrophobic moments (Eisenberg et al. 1982), Fourier transform amphipathic analysis (Finer-Moore and Stroud 1984) and amino acid substitution tables (Donnelly et al. 1993) are valuable tools for identification of amphipathic helical regions in protein sequences. However, they do not take into account possible alternative conformations of flexible polar sidechains. As discussed by e.g. Segrest et al. (1990), there is a requirement for a method of analysis which incorporates such effects.

Two more recent approaches to the problem of identifying and quantifying amphipathic helices have been reported. Segrest et al. (1990) used a combination of helical wheel and hydrophobic moment calculations to identify and classify amphipathic helices according to their mean helical hydrophobic moments and their hydrophilic angles (i.e. the angular range of the hydrophilic region on a helical wheel plot). They correlated these parameters with aspects of protein and peptide function such as protein:protein interactions. In an extension of this work they described a series of computer programs for analysis of sequence data which assign helical regions into the appropriate amphipathic classes (Jones et al. 1992). Brasseur (1991) has used an approach related to that employed here in order to evaluate the "molecular hydrophobicity potential" (MHP) around amphipathic helices. The MHP, derived from the work of Furet et al. (1988) and of Fauchère et al. (1988), is displayed using isopotential contours, providing a three-dimensional representation of the *hydrophobic* nature of a helix. Hence a measure of the fraction of the helix surface which is hydrophilic may be obtained, albeit indirectly. This procedure was used to define different classes of lipid-interacting helices (Brasseur 1991).

The rationale underlying the current study is somewhat different from those described above. The overall aim of our analysis is to define the centre of the *hydrophilic* face of an amphipathic helix so that preliminary models of channel-forming helix bundles may be constructed (see below; Sansom et al. 1991; Sansom et al. 1993). Thus, rather than evaluation of a molecular hydrophobicity potential, a "hydrophilicity potential", i.e. the interaction of a water molecule with the helix surface, has been evaluated. This method is thus related to the GRID program of Goodford (1985). In adopting a molecular mechanics based procedure, a compromise has been effected between the more complete description of peptide-water interactions which would be afforded by molecular dynamics simulations (see Teeter 1991), and the desire for computational efficiency, in order that several peptides and peptide conformations may be investigated.

The electrostatic term of the interaction energy has been evaluated using a constant dielectric $\varepsilon = \varepsilon_0$, i.e. *in vacuo*. This neglects screening of electrostatic interactions by other solvent molecules. A simple method to simulate screening is to use a distance-dependent dielectric ($\varepsilon = \varepsilon_0 r$), thus reducing the magnitude of longer range interactions. This method, which has been criticised on theoretical grounds (Rogers 1986), had relatively minor effects on hydrophilic surface maps. This may be because favourable peptide-water interactions occurred at $r$ values of ca. 2 Å, i.e. at distances for which the effect of screening was small.

The effects of alternative sidechain conformations have been investigated by calculating hydrophilic surface maps for: *a*) five representative $\delta$-toxin structures generated by the simulate annealing protocol; *b*) three different alamethicin molecules (A, B and C) present within the asymmetric unit of the crystal (Fox and Richards 1982); and *c*) three different conformations of the serine sidechains in models of the LS1 peptide. In all three examples the results suggest that changes in polar sidechain conformations may result in shifts in the centre of the hydrophilic face of an amphipathic helix of the order of 60°. Thus, analysis of the effects of sidechain flexibility is clearly of crucial importance when generating initial models of channel-forming helix bundles.

### *Models of ion channel formation*

Current models of channel formation by amphipathic helical peptides (Chung et al. 1990; Sansom 1991) suggest that in the absence of a transbilayer voltage CFPs lie at the membrane:water interface with the helix axis perpendicular to the bilayer normal. On application of a transbilayer voltage, the helices re-orient so that they lie parallel to the bilayer normal, and self-assemble to form a bundle of parallel helices surrounding a central ion-permeable pore.

Generation of an initial model of a bundle of CFP helices requires rotation of the helices about their axes such that the centre of the hydrophilic face of each helix is directed towards the central pore. Analysis of hydrophilic surface maps helps to remove an element of subjectivity present in earlier modelling studies (Sansom et al. 1991). In particular it permits generation of *families* of initial models which may then be refined by further application of simulated annealing (Kerr et al. manuscript in preparation). To date, we have employed hydrophilic surface map data to aid modelling of ion channels formed by the peptaibol CFP zervamicin-II-B (Sansom et al. 1992) and by the influenza A virus M2 protein (Sansom and Kerr 1993).

Overall, we have demonstrated an empirical method for the calculation of hydrophilic surfaces of amphipathic $\alpha$-helices. The method provides support for current models of ion channel formation, and may be used to develop initial models of ion channels. Current studies are centred about development of objective and automatic procedures for the refinement of such models.

*Acknowledgements.* This work was supported by a grant from the Wellcome Trust. IDK is a SERC/CASE student with Shell Research Ltd.

## References

Bernstein F, Koetzle T, Williams G, Meyer E, Brice M, Rodgers J, Kennard O, Shimanouchi T, Tasumi M (1977) The Protein Data Bank: a computer-based archival file for macromolecular structures. J Mol Biol 112:535–542

Brasseur R (1991) Differentiation of lipid-associating helices by use of three-dimensional molecular hydrophobicity potential calculations. J Biol Chem 266:16120–16127

Brooks BR, Bruccoleri RE, Olafson BD, States DJ, Swaminathan S, Karplus M (1983) CHARMM: a program for macromolecular energy, minimization, and dynamics calculations. J Comp Chem 4:187–217

Brünger, AT (1992) X-PLOR, Version 3.0, A system for X-ray crystallography and NMR. Yale University Press, New Haven, CT

Chung LA, DeGrado WF, Lear JD (1990) Orientation of a model ion channel peptide in lipid vesicles. Biophys J 57:462a

Donnelly D, Overington JP, Ruffle SV, Nugent JHA, Blundell TL (1993) Modelling α-helical transmembrane domain: The calculation and use of substitution tables for lipid-facing residues. Protein Sci 2:55–70

Eisenberg D (1984) Three-dimensional structure of membrane and surface proteins. Annu Rev Biochem 53:595–623

Eisenberg D, Weiss RM, Terwilliger TC (1982) The helical hydrophobic moment: a measure of the amphiphilicity of a helix. Nature 299:371–374

Fauchère J-L, Quarendon P, Kaetterer L (1988) Estimating and representing hydrophobicity potential. J Mol Graphics 6:202–206

Finer-Moore J, Stroud RM (1984) Amphipathic analysis and possible formation of the ion channel in an acetylcholine receptor. Proc Natl Acad Sci, USA 81:155–159

Fitton JE (1981) Physicochemical studies on delta haemolysin, a *Staphylococcal* cytolytic peptide. FEBS Lett 130:257–260

Fox RO, Richards FM (1982) A voltage-gated ion channel model inferred from the crystal structure of alamethicin at 1.5 Å resolution. Nature 300:325–330

Furet P, Sele A, Cohen NC (1988) 3D molecular lipophilicity potential profiles: a new tool in molecular modelling. J Mol Graphics 6:182–189

Goodford PJ (1985) A computational procedure for determining energetically favorable binding sites on biologically important macromolecules. J Med Chem 28:849–857

Gray TM, Matthews BM (1984) Intrahelical hydrogen bonding of serine, threonine and cysteine residues within α-helices and its relevance to membrane-bound proteins. J Mol Biol 175:75–81

Haris PI, Ramesh B, Sansom MSP, Kerr ID, Srai KS, Chapman D (1993) Studies of the pore forming domain of a voltage-gated potassium channel protein. Protein Eng (submitted for publication)

Janin J, Wodak S, Levitt M, Maigret B (1978) Conformation of amino acid side-chains in proteins. J Mol Biol 125:357–386

Jones MK, Anantharamaiah GM, Segrest JP (1992) Computer programs to identify and classify amphipathic α helical domains. J Lipid Res 33:287–296

Jorgensen WL, Chandresekhar J, Madura JD, Impey RW, Klein ML (1983) Comparison of simple potential functions for simulating liquid water. J Chem Phys 79:926–935

Kraulis PJ (1991) MOLSCRIPT: a program to produce both detailed and schematic plots of protein structures. J Appl Crystallogr 24:946–950

Lear JD, Wasserman ZR, DeGrado WF (1988) Synthetic amphiphilic peptide models for protein ion channels. Science 240:1177–1181

Lee KH, Fitton JE, Wüthrich K (1987) Nuclear magnetic resonance investigation of the conformation of δ-haemolysin bound to dodecylphosphocholine micelles. Biochim Biophys Acta 891:144–153

Levy RM, Perahia D, Karplus M (1982) Molecular dynamics of an α-helical polypeptide: temperature dependence and deviation from harmonic behaviour. Proc Natl Acad Sci, USA 79:1346–1350

McGregor MJ, Islam SA, Sternberg MJE (1987) Analysis of the relationship between side-chain conformation and secondary structure in globular proteins. J Mol Biol 198:295–310

Mellor IR, Thomas DH, Sansom MSP (1988) Properties of ion channels formed by *Staphylococcus* aureus δ-toxin. Biochim Biophys Acta 942:280–294

Morris AL, MacArthur MW, Hutchinson EG, Thornton JM (1992) Stereochemical quality of protein structure coordinates. Proteins 12:345–364

Nilges M, Brünger AT (1991) Automated modeling of coiled coils: application to the GCN4 dimerization region. Prot Eng 4:649–659

Nilges M, Brünger AT (1993) Successful prediction of the coiled coil geometry of the GCN4 leucine zipper domain by simulated annealing: comparison ot the x-ray structure. Proteins 15:133–146

Nilges M, Clore GM, Gronenborn AM (1988) Determination of three-dimensional structures of proteins from interproton distance data by dynamical simulated annealing from a random array of atoms. Circumventing problems associated with folding. FEBS Lett 239:129–136

Oiki S, Madison V, Montal M (1990) Bundles of amphipathic transmembrane α-helices as a structural motif for ion conducting channel proteins: studies on sodium channels and acetylcholine receptors. Proteins 8:226–236

Richardson JS, Richardson DC (1989) Principles and patterns of protein conformation. In: Fasman GD (ed) Prediction of protein structure and the principles of protein conformation. Plenum Press, New York, pp 1–98

Rogers NK (1986) The modelling of electrostatic interactions in globular proteins. Prog Biophys Mol Biol 48:37–66

Sansom MSP (1991) The biophysics of peptide models of ion channels. Prog Biophys Mol Biol 55:139–235

Sansom MSP (1992a) Proline residues in transmembrane helices of channel and transport proteins: a molecular modelling study. Protein Eng 5:53–60

Sansom MSP (1992b) The roles of serine and threonine sidechains in ion channels: a modelling study. Eur Biophys J 21:281–298

Sansom MSP (1993) Alamethicin and related peptaibols – model ion channels. Eur Biophys J (submitted for publication)

Sansom MSP, Kerr ID (1993) Influenza virus $M_2$ protein: A molecular modelling study of the ion channel. Prot Eng 6:65–74

Sansom MSP, Kerr ID, Mellor IR (1991) Ion channels formed by amphipathic helical peptides – a molecular modelling study. Eur Biophys J 20:229–240

Sansom MSP, Balaram P, Karle IL (1993) Ion channel formation by zervamicin-II-B: a molecular modelling study. Eur Biophys J 21:369–383

Schiffer M, Edmundson AB (1967) Use of helical wheels to represent the structures of protein and to identify segments with helical potential. Biophys J 7:121–135

Segrest JP, De Loof H, Dohlman JG, Brouillette CG, Anantharamaiah GM (1990) Amphipathic helix motif: Classes and properties. Proteins 8:103–117

Stroud RM, McCarthy MP, Shuster M (1990) Nicotinic acetylcholine receptor superfamily of ligand gated ion channels. Biochemistry 29:11007–11023

Tappin MJ, Pastore A, Norton RS, Freer JH, Campbell ID (1988) High-resolution $^1$H NMR study of the solution structure of δ-haemolysin. Biochemistry 27:1643–1647

Teeter MM (1991) Water-protein interactions: Theory and Experiment. Annu Rev Biophys Biophys Chem 20:577–600

Thiaudière E, Siffert O, Talbot J-C, Bolard J, Alouf JE, DuFourcq J (1991) The amphipathic α-helix concept. Consequences on the structure of *Staphylococcal* δ-toxin in solution and bound to lipids. Eur J Biochem 195:203–213

Treutlein HR, Lemmon MA, Engelmann DM, Brunger AT (1992) The glycophorin A transmembrane domain dimer: sequence-specific propensity for a right-handed supercoil of helices. Biochemistry 31:12726–12733

Unwin N (1989) The structure of ion channels in membranes of excitable cells. Neuron 3:665–676

Villarroel A, Herlitze S, Koenen M, Sakmann B (1991) Location of a threonine residue in the α-subunit M2 transmembrane segment that determines the ion flow through the acetylcholine receptor channel. Proc R Soc London Ser B 243:69–74

Woolley GA, Wallace BA (1992) Model ion channels: gramicidin and alamethicin. J Membr Biol 129:109–136